



Science Arts & Métiers (SAM)

is an open access repository that collects the work of Arts et Métiers Institute of Technology researchers and makes it freely available over the web where possible.

This is an author-deposited version published in: <https://sam.ensam.eu>
Handle ID: <http://hdl.handle.net/10985/24882>

To cite this version :

Adil EL BAROUDI, Jean Yves LE POMMELLE, Vincent COUANET - Love waves propagation in layered viscoelastic waveguides characterized by a Zener model - Sensors and Actuators: A. Physical - Vol. 369, p.8 - 2024

Any correspondence concerning this service should be sent to the repository

Administrator : scienceouverte@ensam.eu



Love waves propagation in layered viscoelastic waveguides characterized by a Zener model

A. El Baroudi^{*}, J.Y. Le Pommellec, V. Couanet

LAMPA, Arts et Metiers Institute of Technology, 2 bd du Ronceray, 49035 Angers, France

Keywords:

Love waves
Viscoelastic material
Zener model
Creep and relaxation phenomena
Analytical approach

A B S T R A C T

This paper describes a theory of surface Love waves propagating in lossy waveguides consisting of a viscoelastic layer deposited on a semi-infinite elastic substrate. The Zener model to describe the viscoelastic behavior of a medium is used. This simple model captures both the relaxation and retardation. A new form of the unsteady momentum equation for viscoelastic waveguides has been established. By using appropriate boundary conditions, an analytical expression for the complex dispersion equation of Love waves has been deduced. The influence of the loss factor and the ratio of shear moduli of the surface layer on the dispersion curves of Love waves velocity and attenuation is analyzed numerically. The numerical solutions show the dependence of the velocity change and the wave attenuation in terms of the loss factor and the ratio of shear moduli. The obtained results show that the change in the ratio of shear moduli can represent a hardening or softening effect of the surface layer. These effects depend on the loss factor value of the surface layer. In addition, these results are novel, fundamental and can be applied in the characterization of the viscoelastic properties of soft biomaterials and tissues, in nondestructive testing of materials, in geophysics and seismology. Thus, the obtained complex dispersion equation can be very useful to interpret the experimental measurements of Love waves properties in viscoelastic waveguides.

1. Introduction

There is an increasing demand of highly sensitive analytical techniques in the fields of biotechnology [1], ultrasonic coatings protection [2], medical diagnostics [3] and chemistry [4]. Optical and acoustic waves sensing technologies are currently used [5]. In particular, the Love wave acoustic sensors have attracted increasing attention from the scientific community during the last two decades, due to their reported high sensitivity to the surrounding environment. Various scientific and engineering domains implied Love waves, such as viscosity sensors [6–17], nondestructive testing and material characterization [18–22], geophysics and seismology [23–28], etc.

Love wave is a transverse surface wave having one component of mechanical displacement, parallel to the surface and perpendicular to the direction of wave propagation. The Love wave sensor is a layered structure formed by a piezoelectric substrate and a guiding layer [8, 12, 29]. In addition, the condition for the existence of Love waves is that the bulk transverse wave velocity in the layer is lower than that in the substrate. The difference between the mechanical properties of the guiding layer and the substrate creates an entrapment of the acoustic energy in the guiding layer keeping the wave energy near the surface [30]. The confinement of the wave in the guiding layer makes

Love wave devices very sensitive towards any changes occurring on the sensor surface [31].

Classical Love waves were initially analyzed in lossless waveguides, consisting of an elastic surface layer deposited on an elastic substrate. As a result, the wave number of the Love wave was real and the wave propagated unattenuated, i.e., its amplitude was constant as a function of the propagation distance. Very few papers were published up to date on Love waves propagating in lossy waveguides, i.e., in waveguides whose surface layer and/or substrate are lossy. Among these articles we find those of Kielczynski *al.* [32, 33] in which the Love waves properties (phase velocity and attenuation) have been determined analytically where the surface layer is considered as a viscoelastic material which follows the Kelvin-Voigt model. Qualitatively, Kelvin-Voigt model gives retarded elastic behavior and represents a crosslinked polymer. In addition, the Maxwell model gives steady-state creep and would represent an uncrosslinked polymer.

However, most polymers do not exhibit viscoelastic behavior described by the simple Kelvin-Voigt and Maxwell models because the conformational changes and the viscous flow are constrained by a multitude of physical entanglements and chemical crosslinks which impair viscoelastic flow in a very complicated way. The situation is

^{*} Corresponding author.

E-mail address: adil.elbaroudi@ensam.eu (A. El Baroudi).

<https://doi.org/10.1016/j.sna.2024.115209>

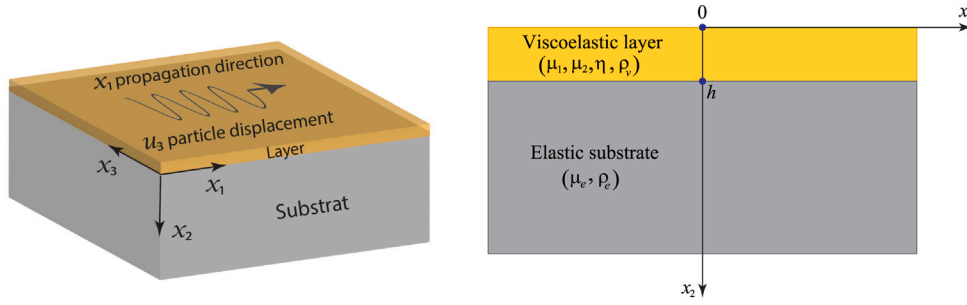


Fig. 1. Waveguide structure geometry (3D and 2D) with a viscoelastic surface layer of thickness h , deposited on an elastic half space. Love waves are polarized along the x_3 axis, they propagate in the x_1 direction and their amplitude decays asymptotically along the x_2 axis. ρ_v , μ_1 , μ_2 and η correspond to the density, shear modulus and viscosity of the surface layer. ρ_e and μ_e the density and shear modulus of the elastic half space.

further complicated if the polymer in question has a complex morphology such as crystalline domains dispersed in an amorphous matrix, microphase separated polymer domains and interpenetrated polymer networks. For these materials, more elaborate spring dashpot models (for example Zener model) have to be employed to effectively describe their complicated viscoelastic behavior. Therefore, the main goal of this article is to use a more elaborate viscoelastic model that captures both the relaxation and retardation in order to evaluate the impact of losses in the surface layer on the propagation characteristics of the Love waves. For this purpose, the generalization of Newton's second law based on Zener's model is necessary. This generalization leads to an analytical model to study this propagation.

2. Description of Love wave surface waveguide

The geometry of the waveguide structure with a viscoelastic (lossy) surface layer of thickness h , deposited on an elastic (lossless) half space is shown in Fig. 1. The mechanical displacement u_3 of the Love wave is directed along the x_3 axis, which is perpendicular to the direction of propagation x_1 and perpendicular to the x_2 axis pointing into the bulk of the substrate. Love wave is a surface wave, hence its mechanical displacement u_3 should vanish in the bulk of the substrate for $x_2 \rightarrow \infty$. It was assumed that the amplitude u_3 is constant along the x_3 axis and the wavefronts are infinitely extended along the x_3 direction. As a result, all partial derivatives over the axis x_3 vanish.

Continuum mechanics assumes that during deformation the material can store elastic energy without losses (dissipation). However, all real materials display some sort of lossy behavior, especially polymers, with a behavior that combines energy storing properties of elastic solids with energy dissipation properties of viscous liquids. Therefore, such materials were named viscoelastic materials.

2.1. Viscoelastic constitutive equation

The model that captures both the relaxation and retardation is known as the three-parameter model. This model is obtained by adding a spring either in series to a Kelvin-Voigt model or in parallel to a Maxwell model (see Fig. 2). This model is sometimes referred to as the Zener Model and is employed to describe a material that will fully recover after a load is removed because the spring connected in parallel to the Maxwell element will continue to move the piston of the dashpot back to its original position. Therefore, the simplest approach to describe viscoelasticity assumes that the material consists of a viscous element and two elastic components.

Viscoelastic properties of the surface layer are described in this paper using Zener model. Therefore, the constitutive equation that describes the relation between force and deformation is expressed in the following form [34]:

$$\mu_1 \tau + \eta \frac{\partial \tau}{\partial t} = 2\mu_1 \mu_2 \epsilon + 2(\mu_1 + \mu_2) \eta \frac{\partial \epsilon}{\partial t} \quad (1)$$

where $\epsilon = [\nabla \mathbf{u} + (\nabla \mathbf{u})^T] / 2$ stands for the strain tensor. Qualitatively, Zener model describes the behavior of a typical polymer. The Kelvin-Voigt model gives retarded elastic behavior and represents a crosslinked polymer. The Maxwell model gives steady-state creep and would represent an uncrosslinked polymer. In addition, with an appropriate choice of μ_1 and μ_2 , the Zener model can represent both types of behavior. Moreover, this mathematical model is used to determine the loss transmission coefficient of a sandwich structure with a viscoelastic core [35–37].

3. Mathematical formulation of the problem

In this section, we establish the partial differential equations describing the Love waves propagation in a viscoelastic surface layer deposited on an elastic substrate in terms of the mechanical displacement. Mathematical analysis begins with linear momentum equation written in its generalized unsteady form for a Zener type viscoelastic constitutive equation. Subsequently, the appropriate boundary conditions are formulated for the shear stress and shear mechanical displacement of the Love wave. The conservation of linear momentum in the absence of the body forces implies:

$$\rho \frac{\partial^2 \mathbf{u}}{\partial t^2} = \nabla \cdot \boldsymbol{\sigma} \quad (2)$$

where \mathbf{u} is the displacement vector, ρ is the density and $\boldsymbol{\sigma}$ is the total stress tensor and can be written as:

$$\boldsymbol{\sigma} = \lambda (\nabla \cdot \mathbf{u}) \mathbf{I} + \boldsymbol{\tau} \quad (3)$$

Here λ is the Lamé's first parameter, \mathbf{I} is the identity tensor and $\boldsymbol{\tau}$ is the shear stress tensor given in Eq. (1). In order to obtain a generalized form of momentum equation for a viscoelastic media, we start by applying the divergence operator to both sides of Eq. (1) and taking into account Eqs. (2) and (3), yields the following generalized unsteady momentum equation:

$$\rho \left(1 + \frac{\eta}{\mu_1} \frac{\partial}{\partial t} \right) \frac{\partial^2 \mathbf{u}}{\partial t^2} = \lambda \left(1 + \frac{\eta}{\mu_1} \frac{\partial}{\partial t} \right) \nabla \nabla \cdot \mathbf{u} + \left[\mu_2 \left(1 + \frac{\eta}{\mu_1} \frac{\partial}{\partial t} \right) + \eta \frac{\partial}{\partial t} \right] (\nabla^2 \mathbf{u} + \nabla \nabla \cdot \mathbf{u}) \quad (4)$$

The Love wave is taken to propagate in the x_1 -direction, with shear displacement in the x_3 -direction. A plane wave in the x_1 -direction is considered, with displacement in x_3 -direction only, $\mathbf{u} = (0, 0, u_3)$. Owing to symmetry, the mechanical displacement should be independent of x_3 , $u_3 = u_3(x_1, x_2)$.

3.1. Viscoelastic surface layer

The component of the mechanical displacement $u_3^{(v)}$ along the x_3 axis of the Love wave in the viscoelastic surface layer is governed by the equation of motion obtained from the second Newton's law as follow:

$$\left[\mu_2 \left(1 + \frac{\eta}{\mu_1} \frac{\partial}{\partial t} \right) + \eta \frac{\partial}{\partial t} \right] \nabla^2 u_3^{(v)} - \rho_v \left(1 + \frac{\eta}{\mu_1} \frac{\partial}{\partial t} \right) \frac{\partial^2 u_3^{(v)}}{\partial t^2} = 0 \quad (5)$$

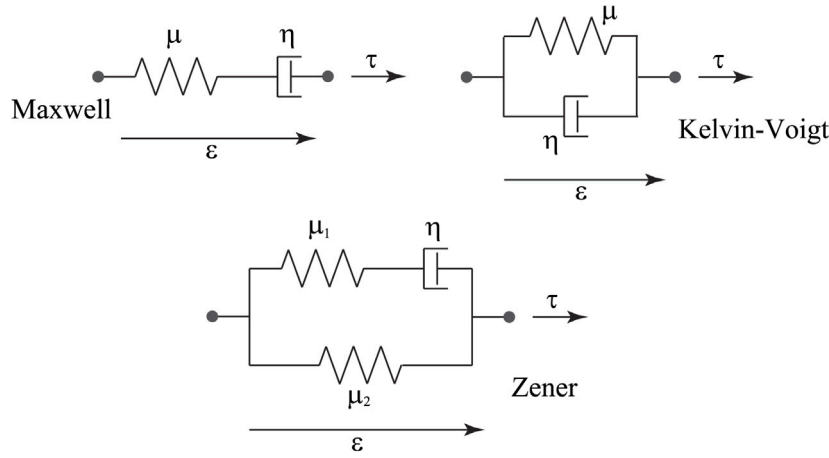


Fig. 2. Maxwell, Kelvin-Voigt and Zener models.

where ∇^2 is the Laplacian operator, ρ_v the density and the superscript (v) is used throughout this paper for the viscoelastic surface layer.

3.2. Elastic substrate

In this work the substrate is considered to be a semi-infinite isotropic elastic medium, and mechanical displacement $u_3^{(e)}$ is governed, using the elastodynamic theory by the Navier's equation:

$$\mu_e \nabla^2 u_3^{(e)} - \rho_e \frac{\partial^2 u_3^{(e)}}{\partial t^2} = 0 \quad (6)$$

where μ_e is the storage shear modulus and ρ_e the density. Note that Eq. (6) can easily be obtained when the viscosity η is set identically to zero in Eq. (5). The superscript (e) will be employed throughout this paper for the elastic substrate.

3.3. Analytical solutions for the equations of motion

In this paper it is assumed that the analyzed Love wave is time harmonic, i.e., its propagation is described by an exponential propagation factor $\exp[j(kx_1 - \omega t)]$, where $j = \sqrt{-1}$, k is the wave number of the Love wave and ω its angular frequency. Since surface layer is viscoelastic the wave number k will be in a complex-value quantity $k = k_r + jk_i$ where the real part k_r determines the Love wave velocity and the imaginary part k_i , is the Love wave attenuation. Moreover, mechanical displacements $u_3^{(v)}$ and $u_3^{(e)}$ of a time-harmonic Love wave, propagating along the x_1 axis, and polarized along the x_3 axis, are sought in the following form:

$$\begin{aligned} u_3^{(v)}(x_1, x_2, t) &= U_v(x_2) e^{j(kx_1 - \omega t)} \\ u_3^{(e)}(x_1, x_2, t) &= U_e(x_2) e^{j(kx_1 - \omega t)} \end{aligned} \quad (7)$$

where $U_v(x_2)$ and $U_e(x_2)$ represent the distribution with the depth of the mechanical displacement in the viscoelastic surface layer and in the substrate, respectively. After substitution of Eq. (7) into equations of motion (5) and (6), one obtains the following differential equations of the second order:

$$\left(\frac{d^2}{dx_2^2} + \beta_v^2 \right) U_v(x_2) = 0, \quad \left(\frac{d^2}{dx_2^2} - \beta_e^2 \right) U_e(x_2) = 0 \quad (8)$$

where β_v and β_e are given in the following form:

$$\beta_v^2 = k_v^2 - k^2, \quad \beta_e^2 = k^2 - k_e^2 \quad (9)$$

in which the wavenumbers k_v and k_e are expressed as:

$$k_v = \frac{\omega}{c_v(\omega)}, \quad k_e = \frac{\omega}{c_e}$$

and $c_v(\omega) = \sqrt{\mu(\omega)/\rho_v}$ is the complex shear wave velocity in the viscoelastic surface layer and $c_e = \sqrt{\mu_e/\rho_e}$ is the shear wave velocity in the elastic substrate. Furthermore, the complex shear modulus $\mu(\omega)$ present in the complex shear wave velocity $c_v(\omega)$ can be defined according to the used viscoelastic constitutive equation as:

$$\frac{\mu(\omega)}{\mu_2} = 1 + \frac{\alpha}{1 + \frac{\alpha^2}{\omega^2 \delta^2}} - j \frac{\omega \delta}{1 + \frac{\omega^2 \delta^2}{\alpha^2}} \quad (10)$$

where the Zener time $\delta = \eta/\mu_2$ characterizes the crossover from elastic to viscous behavior, and $\alpha = \mu_1/\mu_2$ represents the ratio of the shear moduli. By contrast, the shear modulus μ_e of the lossless elastic substrate is a real number and does not depend on the wave frequency. Note that the real part of the complex elastic modulus refers to the storage modulus and its imaginary part to the loss modulus [38,39]. In addition, Eq. (10) shows that the mechanical losses in viscoelastic surface layer, for shear vibrations, can be described by two parameters, i.e., by the loss factor $\delta\omega$ and the shear moduli ratio α . Moreover, since the amplitude of Love waves must tend to zero for $x_2 \rightarrow \infty$, the solution of Eq. (8) can be written in the form of:

$$U_v(x_2) = A_v \cos(\beta_v x_2) + B_v \sin(\beta_v x_2), \quad U_e(x_2) = A_e e^{-\beta_e x_2} \quad (11)$$

where A_v , B_v and A_e are unknown arbitrary amplitudes.

3.4. Boundary conditions and complex dispersion equation

The solution of the Love wave propagation must satisfy the boundary conditions on the waveguide layer ($x_2 = 0$) and the continuity conditions along the interface between the viscoelastic surface layer and the substrate ($x_2 = h$). At the interface $x_2 = h$, the mechanical conditions are continuity of displacement and stress components, i.e. :

$$u_3^{(v)} = u_3^{(e)}, \quad \sigma_{23}^{(v)} = \sigma_{23}^{(e)} \quad (12)$$

The surface of the viscoelastic surface layer is stress-free boundary (i.e., at $x_2 = 0$). This requires:

$$\sigma_{23}^{(v)} = 0 \quad (13)$$

Thus, the stress component in terms of the displacement component along the x_3 axis that will be used in these boundary conditions are given by:

$$\sigma_{23}^{(v)} = \mu(\omega) \frac{\partial u_3^{(v)}}{\partial x_2}, \quad \sigma_{23}^{(e)} = \mu_e \frac{\partial u_3^{(e)}}{\partial x_2} \quad (14)$$

Substitution of the Eqs. (7) and (11) into the boundary conditions (12) and (13) and taking into account the Eq. (14), yields a system of three linear algebraic equations in three undetermined amplitudes. For

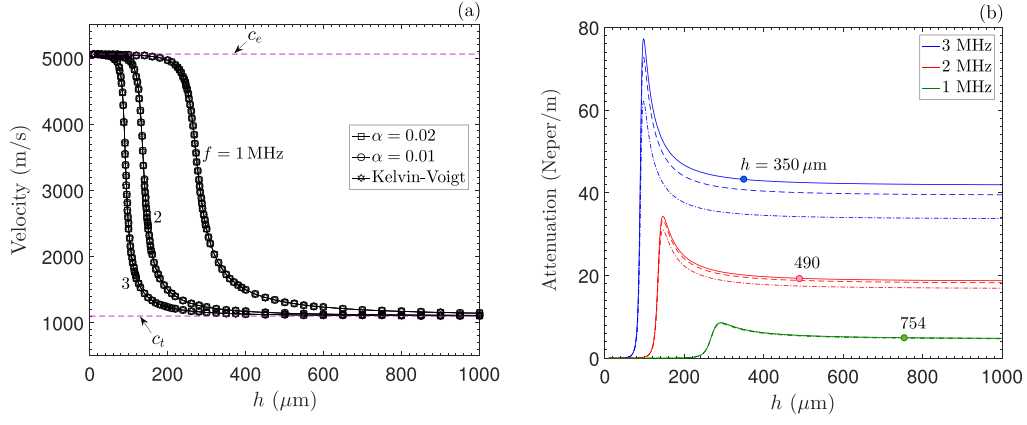


Fig. 3. Love wave velocity and attenuation as function of the surface layer thickness h for three frequencies and constant surface layer viscosity $\eta = 0.37 \text{ Pa} \cdot \text{s}$. In Figure (b): solid lines Kelvin-Voigt, dashed lines $\alpha = 0.02$ and dash-dotted line $\alpha = 0.01$.

nontrivial solutions of the undetermined amplitudes to exist, the determinant of this system has to equal zero, which leads to the following complex dispersion equation of the Love waves:

$$\left[1 + \delta\omega \left(\frac{\xi}{1 + \xi^2} - \frac{j}{1 + \xi^2} \right)\right] \tan(\beta_v h) - \frac{\beta_e \mu_e}{\beta_v \mu_2} = 0 \quad (15)$$

where $\xi = \delta\omega/\alpha$. This equation contains two real-valued unknowns, i.e. the real part k_r and the imaginary part k_i of the complex wave number of the Love wave. The material parameters of the viscoelastic surface layer and elastic substrate, along with the operating frequency of the Love wave and the viscoelastic surface layer thickness, are incorporated in the dispersion equation and treated as parameters of this equation. Otherwise, this equation represents an implicit dispersion equation of Love waves propagating in the waveguide structure (see Fig. 1). This dispersion equation was solved numerically using specialized procedures from the computer package Matlab. Once the complex wavenumber is obtained, the phase velocity is calculated by ω/k_r . While the imaginary part of complex wavenumber describes the attenuation per unit length in the propagation direction. Note that the dispersion equation of the Love wave in an elastic waveguide is obtained by replacing k_v in Eq. (9) by $k_i = \omega/c_t$ where $c_t = \sqrt{\mu_2/\rho_v}$ represents the shear wave velocity in the elastic surface layer. Moreover, knowledge of the phase velocity and attenuation for Love waves propagating in lossy waveguides is indispensable in modeling and design of bio and chemosensors [40], whose sensing surface layer is usually made from a lossy material.

Love waves exhibit a multimode character. In theory, they have an infinite number of modes with different amplitude distributions, phase velocities and cut-off frequencies. However, in many practical applications such as non destructive testing and sensors [41], most important is the fundamental mode with a zero cut-off frequency. Therefore, in this work, the attention is focused on the properties of the fundamental mode of Love waves.

4. Comparison with other studies

In this section, we check the accuracy and numerical robustness of the dispersion equation developed in this work in a particular case. A comparison study is performed for a viscoelastic waveguide characterized by a Kelvin-Voigt model [32]. Thus, same dimensionless parameters that were used by Kielczynski [32] are introduced. Furthermore, when the viscoelastic material is modeled by a simple constitutive equation of the Kelvin-Voigt type, the normalized frequency $\delta\omega$ represents the loss tangent $\tan\theta$ of the material, where θ is the phase angle between the shear stress and shear strain in the material [32]. The normalized frequency also represents the loss factor which is proportional to the ratio of the energy dissipated and the

energy stored for dynamic loading [42]. It was calculated as the ratio of the imaginary part of the complex shear elastic modulus to its real part. The inverse of the loss tangent is equal to the mechanical quality factor Q of the material. Typical values of the loss factor for shear-horizontal surface waves range from 10^{-5} in single-crystal materials to $10^{-3} - 10^{-1}$ in polycrystalline solids and solid polymers [43]. On the other hand, the mechanical quality factor Q for the shear-horizontal surface waves propagating in the upper Earth crust [44], is of the order of $Q = 50$. Thus, the corresponding loss tangent is equal to $2 \cdot 10^{-3}$, a value much lower than 1. For more description, there is an excellent article dedicated to the study of the Love waves characteristics in a viscoelastic medium using the Kelvin-Voigt model [32].

4.1. Love waves velocity and attenuation versus surface layer thickness

Fig. 3 illustrates the dispersion curves of the Love wave velocity and attenuation as function of the surface layer thickness h , for a viscosity of $\eta = 0.37 \text{ Pa} \cdot \text{s}$ and three frequencies namely $f = 1, 2$ and 3 MHz . As it is seen in Fig. 3(a) the Love wave velocity begins at c_e for $h = 0$ and decreases monotonically to the surface layer shear wave velocity c_t . In other words, for thicker waveguide surface, properties of the Love wave are more influenced by properties of the surface layer. Fig. 3(a) also shows that the shear moduli ratio has insignificant effect on the velocity in the case of low values of the loss factor $\delta\omega$. For the three frequencies $f = 1, 2$ and 3 MHz , the values of $\delta\omega$ are respectively $0.0016, 0.0032$ and 0.0048 . In contrast to the velocity, the Love wave attenuation strongly depends on the shear moduli ratio α of the surface layer.

Fig. 3(b) shows a non monotonic behavior of the Love wave attenuation with the surface layer thickness. Indeed, the attenuation has a pronounced maximum as a function of surface layer thickness. For increasing frequencies of the Love wave the maximum occurs for lower surface layer thickness, i.e., for frequencies $f = 1, 2$ and 3 MHz the maximum occurs, respectively, for $h = 292, 146$ and $97 \mu\text{m}$. The maximum of Love waves attenuation as a function of the surface layer thickness was also observed in [14,16,17]. The attenuation observed in these articles are mainly due to the liquid viscosity which loads the surface layer. In the present paper however, attenuation is caused by the viscosity of the viscoelastic surface layer. Fig. 3(b) reveals that the attenuation as function of the surface layer thickness has a plateau region, i.e., for frequencies $f = 1, 2$ and 3 MHz the plateau region begins, respectively, for $h = 754, 490$ and $350 \mu\text{m}$. In addition, the results in Fig. 3 agree very well with those obtained by Kielczynski [32] for Kelvin-Voigt model.

One can observe an important difference between the Kelvin-Voigt and Zener models regarding the maximum of Love waves attenuation. Fig. 4 shows that when the Kelvin-Voigt model is assumed, the maximum of Love waves attenuation is proportional to the square

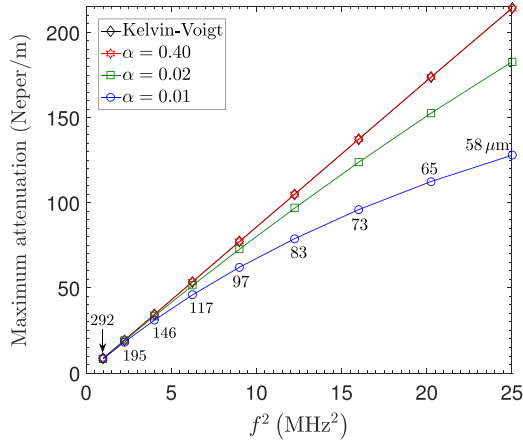


Fig. 4. Maximum of Love waves attenuation and corresponding thickness versus square of the frequency.

of the frequency, with a constant of proportionality equal to 8.5697. Nevertheless, this proportion relationship is considered to fail when the ratio of the shear moduli α of the viscoelastic surface layer is smaller than 0.4.

4.2. Love waves velocity and attenuation versus loss factor

Fig. 5 exhibits the impact of the loss factor of the surface layer on the Love waves velocity and attenuation for three values of surface layer thickness. It can be seen from this figure that the Love waves velocity and attenuation have a same trend, namely they monotonically increase with the increasing loss factor of the surface layer. This monotonic trend reveals a creep behavior of the surface layer. As we will see in Fig. 6, the attenuation evolution is no longer monotonic when the loss factor of the surface layer exceeds the value of 0.8. Fig. 5 also shows that the Love waves velocity decreases with increasing in shear moduli ratio of the surface layer, and however, the attenuation grows with increasing in shear moduli ratio. This increase in the value of ratio of the shear moduli leads to a softening effect on the surface layer stiffness. Moreover, in this range of variation of the loss factor, i.e. from 0 to 0.8, the Zener model perfectly predicts the creep behavior of the surface layer given by the Kelvin-Voigt model for high values of the shear moduli ratio. In addition, the results in Fig. 5 agree exceptionally well with those obtained by Kielczynski [32] for Kelvin-Voigt model.

5. Numerical results and discussion

Having established the accuracy through the comparison study illustrated in Figs. 3 and 5, further numerical results are given in this section. The material properties given in Table 1 for the viscoelastic surface layer and elastic substrate [32] are taken to carry out numerical calculations in the present paper. In this work, numerical calculation is performed for a surface layer thicknesses of $600\mu\text{m}$ and a frequency of 1 MHz. The material parameters presented in Table 1 in the second column correspond to the elastic parameters of PMMA poly(methyl methacrylate). Subsequently, the material parameters given in Table 1 in the third column correspond to the elastic parameters of ST-cut Quartz.

5.1. Love waves characteristics versus loss factor: Comparison of three viscoelastic models

Fig. 6 display the dependence of the Love waves velocity and attenuation on the loss factor of the viscoelastic surface layer for three viscoelastic models, namely Maxwell, Kelvin-Voigt and Zener (Fig. 2).

Table 1

Material parameters used for the waveguide structure.

	Surface layer	Substrate
Shear waves velocity	$c_t = 1100.85$ (m/s)	$c_e = 5060.02$ (m/s)
Storage shear modulus	$\mu_2 = 1.43$ (GPa)	$\mu_e = 67.85$ (GPa)
Density	$\rho_e = 1180$ (kg/m ³)	$\rho_e = 2650$ (kg/m ³)

In this figure, Love waves velocity and attenuation have been plotted over a wide range of variation of the loss coefficient of viscoelastic surface layer. It can be seen from this figure that the Love waves velocity and attenuation do not have a same trend. Velocity monotonically increase with the increasing loss factor of the surface layer and then reaches a plateau region. The increase in the loss factor (i.e. increase in the surface layer viscosity) results in an increase of the Love wave velocity (see Fig. 6(a)). Possible physical explanation for this behavior may be that viscosity increasing causes an apparent stiffening of the viscoelastic surface layer and therefore an increase in its shear modulus. However, the attenuation exhibits a non-monotonic behavior. First, it increases (as Kelvin-Voigt) with the loss factor of the viscoelastic surface layer, passes through a maximum, then decreases (as Maxwell). The increase in attenuation can be interpreted physically by a partial stiffening of the viscoelastic surface due to the increase in its viscosity. Otherwise, the decrease in attenuation can be attributed to a total stiffening of the viscoelastic surface (see Fig. 6(a)). Furthermore, for low values of shear moduli ratio, relaxation phenomenon appears for small values of the loss coefficient of surface layer. Moreover, for high values of the shear moduli ratio, relaxation takes place for larger values of the loss coefficient. In other words, Zener model can be used to simultaneously describe both behaviors namely creep and relaxation. These behaviors are characteristic of complex polymers. These observations which highlight the simultaneous effect of shear moduli ratio and loss factor on Love waves characteristics are in perfect adequacy with the analytical expression of the complex shear modulus given in Eq. (10).

Otherwise, a very important information can be obtained from the curves in Fig. 6. These curves show three behavior zones, namely, creep, relaxation and a transition zone between creep and relaxation. These zones depend on the loss factor of the surface layer, and in each zone the Love wave velocity depends on the ratio of the shear moduli. Firstly, in the first zone (creep) for low values of the loss factor, the velocity decreases when the ratio of the shear moduli increases. In this zone, the increase in the value of ratio of the shear moduli leads to a softening effect on the stiffness of the surface layer. Secondly, in the zone (transition) for intermediate values of the loss factor, the velocity curves intersect. Thirdly, in the third zone (relaxation) for high values of the loss factor, the velocity increases when the ratio of the shear moduli increases. In this zone, the increase in the value of ratio of the shear moduli leads to a hardening on the stiffness of the surface layer.

5.2. Love waves characteristics versus normalized loss factor ξ

In this paragraph, the influence of the ratio of $\delta\omega$ (loss factor) and α (ratio of the shear moduli) on the Love waves velocity and attenuation is depicted in Fig. 7. This Figure highlights the combined effect of the loss factor and the ratio of shear moduli already observed in Fig. 6. The obtained results are consistent with those of Fig. 6.

In Fig. 7(a), the intersection points of the Love wave velocity curves with the velocity axis ($\xi = 0.001$) correspond to the values obtained using the Kelvin-Voigt model. In other words, in the complex dispersion Eq. (15), the complex shear modulus $\mu(\omega)$ should be replaced by $\mu_2(1 - j\omega\delta)$. The Love wave velocity increases with ξ , passes through a maximum and rapidly decreases. This maximum value increases with the loss factor. Thus, the increase in velocity related to creep phenomenon of the viscoelastic surface layer and its decrease corresponds to relaxation. Moreover, all the curves converge towards

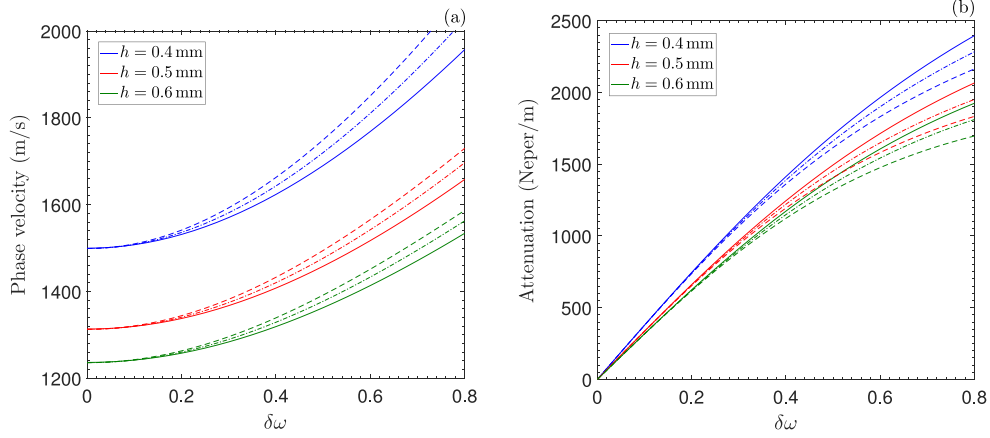


Fig. 5. Love wave velocity and attenuation versus loss factor for three surface layer thicknesses and constant frequency $f = 1$ MHz. This Figure is identical to that of Ref. [32]. Solid lines Kelvin-Voigt, dashed lines $\alpha = 5$ and dash-dotted line $\alpha = 10$.

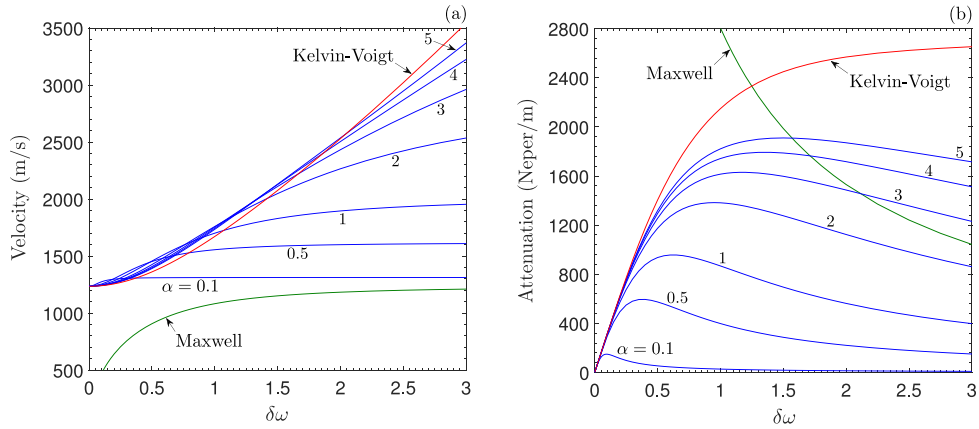


Fig. 6. Love waves velocity and attenuation versus loss factor for three viscoelastic models, a constant surface layer thicknesses 0.6 mm and constant frequency 1 MHz.

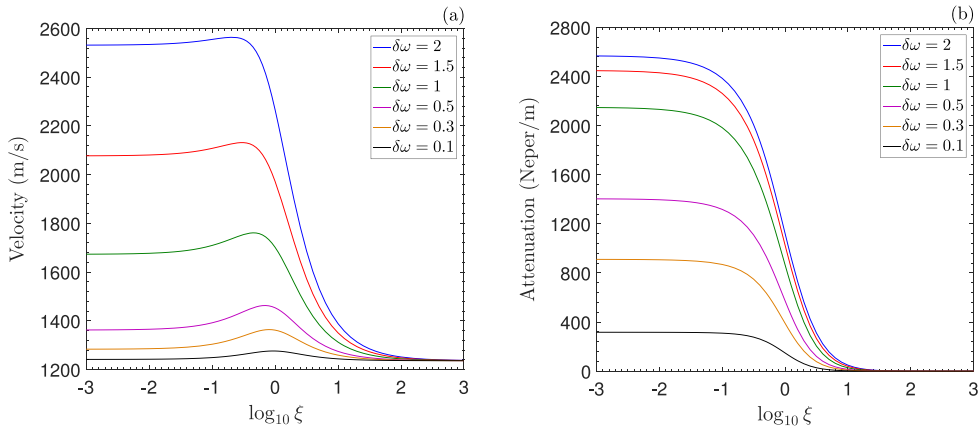


Fig. 7. Love waves velocity and attenuation versus normalized loss factor $\xi = \delta\omega/a$ for a constant surface layer thicknesses 0.6 mm and constant frequency 1 MHz.

the velocity characterizing an elastic waveguide, and in this case the complex shear modulus becomes real, i.e. $\mu(\omega) = \mu_2$. With regard to the attenuation plotted in Fig. 7(b), its behavior is consistent with the trend of Love wave velocity. In particular, during relaxation the attenuation decreases and takes the value zero when the waveguide is elastic. In summary, Love wave velocity and attenuation curves show the transition between the phenomena of creep and relaxation. Zener's model highlights this transition. Also, this transition is strongly depend to the values of the loss factor and the ratio of the shear moduli of the viscoelastic surface layer.

6. Comparison of two standard linear solid model configurations

As mentioned previously, the model that captures both the relaxation and retardation is known as the three-parameter model or standard linear solid (SLS) model. The first configuration of this model is obtained by adding a spring in parallel to a Maxwell model (see Fig. 2). This model is sometimes referred to as the Zener Model. The second configuration is obtained by adding a spring in series to a Kelvin-Voigt model (see Fig. 8). This model is sometimes referred to

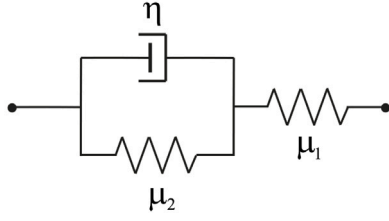


Fig. 8. Standard linear solid model with Kelvin-Voigt configuration.

as the Poynting-Thomson model. A comparison between these two configurations is made in this section.

Using equilibrium and compatibility conditions for the Poynting-Thomson model (see Fig. 8), the viscoelastic constitutive equation (1) becomes:

$$(\mu_1 + \mu_2) \boldsymbol{\tau} + \eta \frac{\partial \boldsymbol{\tau}}{\partial t} = 2\mu_1 \mu_2 \boldsymbol{\epsilon} + 2\mu_1 \eta \frac{\partial \boldsymbol{\epsilon}}{\partial t}$$

In this case the generalized unsteady momentum equation (4) takes the following form:

$$\rho \left(1 + \frac{\eta}{\mu_1} \frac{\partial}{\partial t} + \frac{\mu_2}{\mu_1} \right) \frac{\partial^2 \mathbf{u}}{\partial t^2} = \lambda \left(1 + \frac{\eta}{\mu_1} + \frac{\mu_2}{\mu_1} \frac{\partial}{\partial t} \right) \nabla \nabla \cdot \mathbf{u} + \left(\mu_2 + \eta \frac{\partial}{\partial t} \right) (\nabla^2 \mathbf{u} + \nabla \nabla \cdot \mathbf{u}) \quad (16)$$

Therefore, Eq. (16) for the Love wave can be written as:

$$\left(\mu_2 + \eta \frac{\partial}{\partial t} \right) \nabla^2 u_3^{(v)} - \rho_v \left(1 + \frac{\eta}{\mu_1} \frac{\partial}{\partial t} + \frac{\mu_2}{\mu_1} \right) \frac{\partial^2 u_3^{(v)}}{\partial t^2} = 0$$

For harmonic behavior, the complex shear modulus given in Eq. (10) can be expressed as:

$$\frac{\mu(\omega)}{\mu_2} = \frac{1 + \frac{1 + \omega^2 \delta^2}{\alpha}}{\left(1 + \frac{1}{\alpha} \right)^2 + \frac{\omega^2 \delta^2}{\alpha^2}} - j \frac{\omega \delta}{\left(1 + \frac{1}{\alpha} \right)^2 + \frac{\omega^2 \delta^2}{\alpha^2}} \quad (17)$$

To plot the Love wave properties in the case of the Poynting-Thomson model, the complex shear modulus (Eq. (17)) is introduced into the dispersion Eq. (15).

In this paragraph, Fig. 9 shows the influence of the model used on the Love waves velocity and attenuation. Velocity and attenuation are plotted against the loss factor of the viscoelastic surface layer for two SLS models, namely Poynting-Thomson and Zener. In this Figure, velocity and attenuation have been plotted over a wide range of variation of the loss factor, and for three values of the shear moduli ratio. The attenuation behavior in the case of Poynting-Thomson model is similar to that of Zener model. However, the amplitude and positions of local maxima are different. Conversely, the model impacts significantly the Love wave velocity. Unlike the Zener model, Poynting-Thomson model does not generate the three behavior zones discussed in section 5.1. The velocity increases when the ratio of the shear moduli increases for each value of the loss factor. The increase in the value of ratio of the shear moduli leads to a hardening on the stiffness of the surface layer.

7. Conclusion

In this paper, Love wave propagation in viscoelastic waveguide is investigated using an original analytical approach. A generalized analytical form of the complex dispersion equation was developed for a viscoelastic model of Zener type. Therefore, the curves highlighting the behavior of attenuation and velocity of Love waves as operating frequency, thickness, ratio of the shear moduli and loss factor of the viscoelastic surface layer were obtained. The obtained results can be very useful in the design and optimization of Love wave sensors.

Generally, the properties of the viscoelastic material can be described by a simple standard linear model, which predicts either relaxation or creep behavior. An important contribution of this article is the use of a viscoelastic model of Zener type able of predicting creep, relaxation and the transition between these two behaviors. These characteristics of dispersion curves are original and can be particularly useful in the design of biosensors, viscosity sensors and chemosensors based on the Love waves. From the performed analysis and numerical calculations, one can conclude that:

- Dispersion curves for the Love wave attenuation reveal a maximum as a function of the surface layer thickness as shown in Fig. 3(b). For a given frequency, there exists a thickness for which the attenuation factor attains the maximum. The amplitude of this maximum strongly depends on the value of the shear moduli ratio.
- For low values of the loss factor in the creep zone as shown in Fig. 5(a), the increase in the viscosity η of the viscoelastic surface layer (and consequently also an increase in the loss factor $\delta\omega$ of the viscoelastic surface layer) results in an increase of the Love wave velocity. This is due to the viscosity of the layer, that causes an apparent stiffening of the material in the layer and an increase in the effective shear stiffness coefficient. Furthermore, the velocity decreases when the ratio of the shear moduli α increases. This increase in the value of ratio of the shear moduli leads to a softening effect on the stiffness of the surface layer. From numerical calculations it follows that the Love wave velocity can significantly increase, even by 39.6%, e.g., for the shear moduli ratio $\alpha = 5$, the thickness $h = 0.4$ mm, the frequency $f = 1$ MHz and $\delta\omega = 0.8$, the Love wave velocity increases from 1499.67 m/s to 2093.89 m/s.
- The Love wave attenuation curves show three behavior zones, namely, creep, relaxation and a transition zone between creep and relaxation, see 6(b). These zones depend on the loss factor of the surface layer, and in each zone the Love wave velocity depends on the ratio of the shear moduli. Unlike the Kelvin-Voigt model, the Love wave attenuation depends approximately linearly on the tangent loss factor of the surface layer and saturates for growing losses.
- The attenuation behavior in the case of Poynting-Thomson model is similar to that of Zener model. However, the amplitude and positions of local maxima are different. Also, Poynting-Thomson model does not generate the three behavior zones for Love wave velocity.

This work is original contribution to the state of the art. Since it covers Love waves characteristics in layered viscoelastic waveguides characterized by a Zener model, the results obtained can be used in many fields of science and technology, such as geophysics and non-destructive testing, and very useful to interpret the experimental measurements of Love waves properties in viscoelastic waveguides.

CRedit authorship contribution statement

A. El Baroudi: Writing – review & editing, Writing – original draft, Project administration, Methodology, Investigation. **J.Y. Le Pommellec:** Writing – review & editing, Investigation, Resources. **V. Couanet:** Writing – review & editing, Resources, Software.

Declaration of competing interest

The authors declare that they have no known competing financial interests or personal relationships that could have appeared to influence the work reported in this paper.

Data availability

No data was used for the research described in the article.

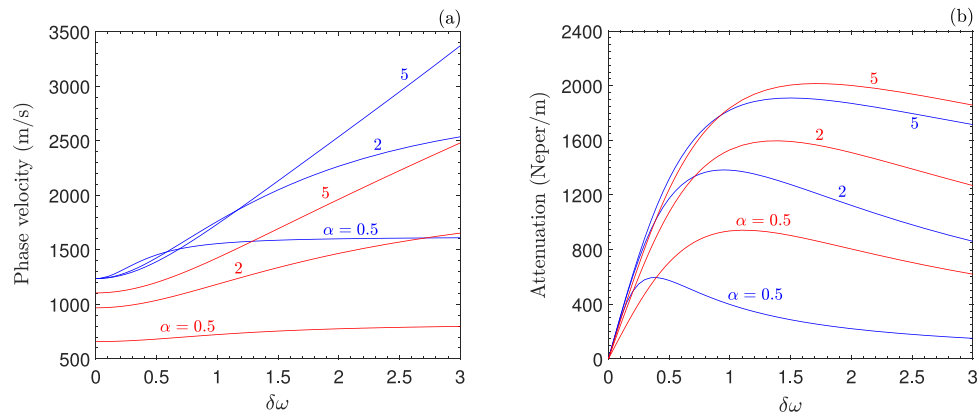


Fig. 9. Love wave properties versus loss factor for a surface layer thicknesses of 0.6 mm. Blue lines represent Zener model and red lines for Poynting-Thomson model. (For interpretation of the references to color in this figure legend, the reader is referred to the web version of this article.)

References

- [1] D. Matatagui, J.L. Fontecha, M.J. Fernandez, I. Gracia, C. Cane, J.P. Santos, M.C. Horrillo, Love-wave sensors combined with microfluidics for fast detection of biological Warfare agents, *Sensors* 14 (7) (2014) 12658–12669.
- [2] F. Guo, J.H. Wu, Mechanism and prediction models for interfacial shear separation of claddings excited by Love waves, *Adv. Mech. Eng.* 13 (3) (2021) <http://dx.doi.org/10.1177/16878140211005196>.
- [3] F. Zhang, S. Li, K. Cao, P. Wang, Y. Su, X. Zhu, Y. Wan, A microfluidic Love-wave biosensing device for PSA detection based on an aptamer beacon probe, *Sensors* 15 (6) (2015) 13839–13850.
- [4] F. Josse, F. Bender, R.W. Cernose, Guided shear horizontal surface acoustic wave sensors for chemical and biochemical detection in liquids, *Anal. Chem.* 73 (24) (2001) 5937–5944.
- [5] M.I.G. Rocha, Y. Jimenez, F.A. Laurent, A. Arnau, Love wave biosensors: A review, *IntechOpen* (2013) 277–310.
- [6] M. Weiss, W. Welsch, M.V. Schickfus, S. Hunklinger, Viscoelastic behavior of antibody films on a shear horizontal acoustic surface wave sensor, *Anal. Chem.* 70 (14) (1998) 2881–2887.
- [7] W. Wang, S. He, A Love wave reflective delay line with polymer guiding layer for wireless sensor application, *Sensors* 8 (12) (2008) 7917–7929.
- [8] P. Kielczynski, M. Szalewski, A. Balcerzak, Effect of a viscous liquid loading on Love wave propagation, *Int. J. Solids Struct.* 49 (17) (2012) 2314–2319.
- [9] J. Liu, A simple and accurate model for Love wave based sensors: Dispersion equation and mass sensitivity, *AIP Adv.* 4 (2014) 077102.
- [10] J.O. Kim, The effect of a viscous fluid on Love waves in a layered medium, *J. Acoust. Soc. Am.* 91 (6) (2014) 3099–3103.
- [11] P. Kielczynski, M. Szalewski, A. Balcerzak, Inverse procedure for simultaneous evaluation of viscosity and density of Newtonian liquids from dispersion curves of Love waves, *J. Appl. Phys.* 116 (4) (2014) 044902.
- [12] A. El Baroudi, Influence of poroelasticity of the surface layer on the surface Love wave propagation, *J. Appl. Mech.* 85 (2018) 051002–1–7.
- [13] P. Kielczynski, Surface waves - New trends and developments, properties and applications of Love surface waves in seismology and biosensors, *IntechOpen* (2018) 17–31.
- [14] A. El Baroudi, J.Y. Le Pommellec, Viscoelastic fluid effect on the surface wave propagation, *Sensors Actuators A* 291 (2019) 188–195.
- [15] P. Kielczynski, M. Szalewski, A. Balcerzak, K. Wieja, Dispersion curves of Love waves in elastic waveguides loaded with a newtonian liquid layer of finite thickness, *Arch. Acoust.* 45 (1) (2020) 19–27.
- [16] A. El Baroudi, J.Y. Le Pommellec, Surface wave in a Maxwell liquid-saturated poroelastic layer, *Appl. Acoust.* 159 (2020) 107076.
- [17] F. Billon, A. El Baroudi, Mathematical modelling of Love waves propagation in viscoelastic waveguide loaded with complex fluids, *Appl. Math. Model.* 96 (2021) 559–569.
- [18] P. Kielczynski, Attenuation of Love waves in low-loss media, *J. Appl. Phys.* 82 (12) (1997) 5932–5937.
- [19] P. Kielczynski, M. Szalewski, An inverse method for determining the elastic properties of thin layers using Love surface waves, *Inverse Probl. Sci. Eng.* 19 (1) (2011) 31–43.
- [20] P. Kielczynski, M. Szalewski, A. Balcerzak, K. Wieja, Group and phase velocity of Love waves propagating in elastic functionally graded materials, *Arch. Acoust.* 40 (2) (2015) 273–281.
- [21] N. Huang, E. Sun, R. Zhang, B. Yang, J. Liu, T. Lü, L. Han, W. Cao, Temperature dependence of normalized sensitivity of Love wave sensor of unidirectional carbon fiber epoxy composite on Mn-Doped 0.24PIN-0.46PMN-0.30PT single crystal substrate, *Appl. Sci.* 10 (23) (2020) 8442.
- [22] P. Kielczynski, Sensitivity of Love surface waves to mass loading, *Sensors Actuators A* 338 (2022) 113465.
- [23] Y. Luo, J. Xia, Y. Xu, C. Zeng, J. Liu, Finite-difference modeling and dispersion analysis of high-frequency Love waves for near-surface applications, *Pure Appl. Geophys.* 167 (2010) 1525–1536.
- [24] L. Hamimu, M. Nawawi, J. Safani, Utilization of multimode Love wave dispersion curve inversion for geotechnical site investigation, *J. Geophys. Eng.* 8 (2) (2011) 341–350.
- [25] T. Boxberger, M. Picozzi, S. Parolai, Shallow geology characterization using Rayleigh and Love wave dispersion curves derived from seismic noise array measurements, *J. Appl. Geophys.* 75 (2) (2011) 345–354.
- [26] Y. Pan, J. Xia, Y. Xu, L. Gao, Z. Xu, Love-wave waveform inversion in time domain for shallow shear-wave velocity, *Geophysics* 81 (2016) 1–14.
- [27] B. Mi, J. Xia, C. Shen, L. Wang, Dispersion energy analysis of Rayleigh and Love waves in the presence of low-velocity layers in near-surface seismic surveys, *Surv. Geophys.* 39 (2018) 271–288.
- [28] A. Negi, A.K. Singh, S. Koley, On the scattering of Love waves in a layered transversely isotropic irregular poro-viscoelastic composite rock structure, *J. Earthq. Eng.* 22 (2) (2022) <http://dx.doi.org/10.1080/13632469.2022.2089406>.
- [29] K. Mitsakakis, A. Tsortos, J. Kondoh, E. Gizeli, Parametric study of SH-SAW device response to various types of surface perturbations, *Sensors Actuators B* 138 (2009) 408–416.
- [30] G. Kovacs, A. Venema, Theoretical comparison of sensitivities of acoustic shear wave modes for (bio) chemical sensing in liquids, *Appl. Phys. Lett.* 61 (6) (1992).
- [31] J. Du, G.L. Harding, J.A. Ogilvy, P.R. Dencher, M. Lake, A study of Love-wave acoustic sensors, *Sensors Actuators A* 56 (3) (1996) 211–219.
- [32] P. Kielczynski, Direct Sturm-Liouville problem for surface Love waves propagating in layered viscoelastic waveguides, *Appl. Math. Model.* 53 (2018) 419–432.
- [33] P. Kielczynski, M. Szalewski, A. Balcerzak, K. Wieja, New theoretical model for mass sensitivity of Love wave sensors, *Arch. Acoust.* 46 (1) (2021) 17–24.
- [34] A.F. Bower, *Applied Mechanics of Solids*, CRC Press, 2009.
- [35] M.R. Zarastvand, M. Ghassabi, R. Talebitooti, A review approach for sound propagation prediction of plate constructions, *Arch. Comput. Methods Eng.* 28 (2021) 2817–2843.
- [36] M.R. Zarastvand, M. Ghassabi, R. Talebitooti, Prediction of acoustic wave transmission features of the multilayered plate constructions: A review, *J. Sandw. Struct. Mater.* 24 (1) (2022) 218–293.
- [37] H. Seilsepour, M.R. Zarastv, R. Talebitooti, Acoustic insulation characteristics of sandwich composite shell systems with double curvature: The effect of nature of viscoelastic core, *J. Vib. Control* 29 (5–9) (2023) 1076–1090.
- [38] J.D. Ferry, *Viscoelastic Properties of Polymers*, third ed., Wiley & Sons, 1980.
- [39] R.G. Larson, *The Structure and Rheology of Complex Fluids*, Oxford University Press, 1999.
- [40] W. Wang, S. He, Theoretical analysis on response mechanism of polymer-coated chemical sensor based Love wave in viscoelastic media, *Sensors Actuators B* 138 (2) (2009) 432–440.
- [41] S. Li, Y. Wan, C. Fan, Y. Su, Theoretical study of monolayer and double-layer waveguide Love wave sensors for achieving high sensitivity, *Sensors* 17 (3) (2017).
- [42] R.S. Lakes, *Viscoelastic Materials*, Cambridge University Press, New York, 2009.
- [43] W.P. Mason, in: S. Flugge (Ed.), *Encyclopedia of Physics*, vol. XI/1, Springer, Berlin, 1961.
- [44] A.L. Jemberie, B.J. Mitchell, Shear wave Q structure and its lateral variation in the crust of China and surrounding regions, *Geophys. J. Int.* 157 (2004) 363–380.